

## Surface texture and luminous analysis of Sol-Gel spin coated Dy-doped ZnO thin films

S. Fathima Thaslin<sup>1</sup>, N.Anandhan<sup>1\*</sup>, A.Amali Roselin<sup>1</sup> K.P.Ganesan<sup>1</sup>, M. Karthikeyan<sup>1</sup>, T. Marimuthu<sup>1</sup>

<sup>1</sup>Advanced Materials and Thin Film Laboratory, Department of Physics, Alagappa University, Karaikudi- 630 003, India.

\*Corresponding author Email: [anandhan\\_kn@rediffmail.com](mailto:anandhan_kn@rediffmail.com)

\*\*\*

**Abstract** - In this present work, we reported and discussed the Pure and Dy (0.01, 0.02 and 0.03 at wt. %)-doped ZnO thin films deposited on a glass substrate using sol-gel spin coating technique at constant 3000rpm for the 30s and annealed at 450°C. As prepared and various concentration of Dy doped films were characterized by X-ray diffraction (XRD), UV-Visible spectroscopy (UV-Vis), Photoluminescence spectroscopy (PL) and Scanning Electron Microscopy (SEM). The XRD pattern showed that all the films are polycrystalline with hexagonal Wurtzite structure and preferentially oriented predominantly along the (101), (002) and (100) growth planes. All the prepared films exhibited low magnitude of transmittance (10 to 40%) in the UV visible range and above 450nm, the optical band gap values decreased from 3.214 to 3.053 eV with increasing doping concentration whereas the average crystalline size decreased from 36.47 to 16.46nm. The PL spectra of ZnO and Dy doped films showed a broad and intensive peak at 384nm (violet emission) is more intense than the peaks at 432nm, 413nm (violet emission) and 470nm (blue emission). The SEM micrographs indicated that the pure ZnO films have wrinkle structure, and the doped ZnO films show homogeneous root-like morphology.

**Key Words:** Zinc Oxide, Spin coating method, Dy-doping.

### 1. INTRODUCTION

ZnO is considered as a very promising functional electronic material due to its electrical, optoelectronic and luminescent properties [1]. ZnO is a group II-VI wide direct band gap (~3.37eV) semiconductor with a large exciton binding energy of 60meV at room temperature and hexagonal Wurtzite structure with lattice parameters of  $a=b= 3.250\text{\AA}$  and  $c= 5.206\text{\AA}$ , then it has attracted much attention because of its numerous prospective applications in many fields [2,3]. Especially, modified ZnO can be used as gas sensors, actuators, piezoelectric transducers, varistors [4], laser diodes, photoconductive UV detectors and high frequency surface acoustic wave (SAW) device [5]. Recently, few scientific team interested to fabricate in ZnO-based thin

films as flat-panel displays (FPDs) and photovoltaic applications, such as the anodic electrode of organic light emitting device (OLED) displays, the active channel layer of thin film transistors (TETs) and the transparent electrode window layer of thin film solar cells [6,7]. The ultraviolet radiation from the excited ZnO thin film is detected, which makes it possible to manufacture ultraviolet laser devices. This kind of short wave laser device will be a substitute for infrared laser memory. In addition, various light emitting devices such as blue light, green light and purple light can be produced by ZnO films [4].

Therefore, many technologies have been developed to fabricate ZnO films, such as reactive magnetron sputtering, the filtered cathodic vacuum arc (FCVA) technique, plasma assisted molecular beam Epitaxy (PMBE), pulsed laser deposition [8], buffer assisted pulsed laser deposition [6], solid state reaction method [9], co-precipitation method, metal organic chemical vapor deposition (MOCVD), spray pyrolysis technique and the sol-gel route. However, the sol-gel method provides the greatest possibility of synthesizing homogeneous and large area oxide films with low costs, low crystallization temperatures and high vacuum -free conditions [10]. Further, an outstanding merit of the sol-gel method is that the doping concentration of the base materials is facile and exactly controllable.

Substitution of a  $\text{Zn}^{2+}$  ion by rare earth group ions such as  $\text{Sm}^{3+}$ ,  $\text{Ln}^{3+}$ ,  $\text{Eu}^{3+}$ ,  $\text{Tb}^{3+}$ ,  $\text{Nd}^{3+}$  and  $\text{Dy}^{3+}$  will produce extra electrons and improve optical, electrical thermal and magnetic properties [11]. The most commonly used dopant among rare earth element is Dysprosium (Dy), hence in this work, we proposed ZnO and ZnO: Dy thin films deposited by sol-gel spin coating technique and focused on investigating the effect of Dy doping concentration on the structural, morphology the sol-gel method using the spin coating technique.

## 2. MATERIALS AND METHODS

Undoped and Dy doped ZnO films were synthesized by a sol-gel spin coating method. The ZnO films were realized onto glass substrates. Before the fabrication process, the substrates were cleaned using isopropanol (IPA) for eliminating the dust or contaminants and then rinsed with deionized (DI) water. The precursor solution was prepared as follows: Zinc acetate dehydrate  $[Zn(CH_3COO)_2 \cdot 2H_2O]$  was dissolved in Isopropyl alcohol  $[(CH_3)_2CHOH]$ , and added were ethanolamine and Dysprosium (III) nitrate pentahydrate  $[Dy(NO_3)_3 \cdot 5H_2O]$  dissolved in (IPA) Isopropyl alcohol as stabilizer and dysprosium dopant source, respectively. The molar ratio of EA to Dy and Zn acetate was maintained at 1.0. These solutions of 0.5M were mixed together in nominal different volume proportions of 1%, 2%, 3%. Each complex solution was stirred for 2h at room temperature until a transparent and homogeneous sol was obtained. The solution was dropped onto glass substrates which were rotated at 3000rpm (rotation per minutes) for the 30s. After depositing by spin coating, the films were dried at 200°C for 10 min into a furnace to evaporate the solvent and remove organic residuals. The process of spin coating and heating were repeated 8 times until the films were formed with a proper thickness and then subsequently annealed at 450°C for 1h in order to crystallize them.

The structure of Dy-doped ZnO film was characterized by (XRD, PAN Analytic X'Pert Pro.) at  $\lambda=1.5406\text{\AA}$ . The photoluminescence (PL) properties were recorded by using Varian Cary Eclipse fluorescence spectrometer with excitation wavelength range about 200-900 nm. Morphological studied and energy dispersive X-ray analyses have been performed with a (Vega 3 Tescan) Scanning electron microscope (SEM) equipped with energy dispersive X-ray analysis (EDAX-Bruker) for getting the elemental chemical analysis. The optical absorbance and transmittance of the films were recorded by a UV-Visible Spectrometer (UV-Vis) (Ocean optics HR 2000) at wavelength range 280 to 1100 nm, and then the optical band gap energy was calculated with.

## 3. RESULTS AND DISCUSSIONS

### 3.1 X-ray Diffraction Analysis

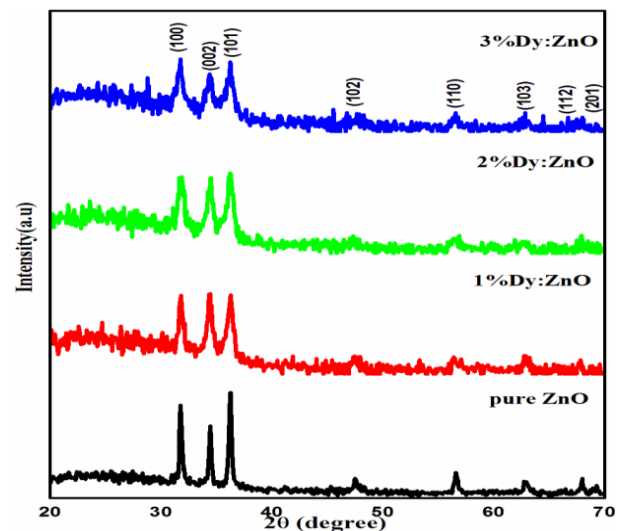


**Fig -1:** XRD patterns of Undoped and Dy-doped ZnO thin films.

X-ray diffraction patterns of pure ZnO and Dy doped ZnO thin films deposited on glass substrate by spin coating technique at 3000 rpm for 30 s and annealed at 450°C shown in fig.1. All films were polycrystalline with hexagonal wurtzite structure, confirmed with International Centre for Diffraction Data (ICDD) card no. 36-1451 [12] and the intense peak at (101) reveals that the crystallites on the films are later growth to the surface of the substrate [13]. When the dopant concentrations are increased, the intensity of diffraction peaks is continuously decreased. It indicates, decreasing the crystallinity of the films with respect to Dy concentrations. These XRD patterns showed that the intensities of diffraction peaks declined as Dy concentration increased (i.e.,) Dy doping within ZnO films caused the crystallinity to degenerate [5].

The crystallite size of pure and Dy doped ZnO films was calculated from the Scherer's formula, dislocation density ( $\delta$ ) and micro strain ( $\mu$ ) were calculated using [7]. As Dy doping content increased, the crystallite size decreased from 36.47nm to 16.46nm. It is ascertained that rare Dy atoms lead to a decrease in the grain size, as a result, it exerts a drag force on boundary motion and grain growth whereas, the micro strain and dislocation density increases for different Dy concentrations [14].

**Table -1:** Crystallite size, Dislocation density and Microstrain for different pure and Dy doped ZnO thin films.

Samples	Crystallite size (nm)	Dislocation Density (lines/m <sup>2</sup> )	Microstrain (lines <sup>-2</sup> /m <sup>-4</sup> )
ZnO	36	1.542	3.01
1%Dy: ZnO	25	2.653	4.52
2%Dy: ZnO	19	3.070	5.54
3%Dy: ZnO	16	7.608	6.37

### 3.2 Photoluminescence spectra analysis

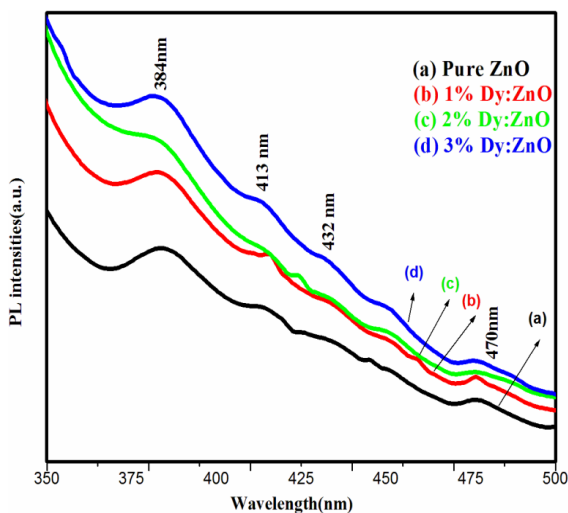


**Fig -2:** Photoluminescence spectra of pure and Dy doped ZnO thin films.

PL spectroscopy was used to study the luminescence properties of thin films. Fig.2 shows PL emission spectra of pure and Dy doped ZnO samples recorded at 320 nm excitation wavelength over the range 350 to 500 nm. The PL spectra of ZnO exhibited, a broad emissions peak at 384nm in the UV region due to a recombination of free excitons and one or more emissions peaks in the visible spectral range, it is accepted that the visible luminescence mainly originates from defect states such as Zn interstitials and oxygen vacancy. All films exhibit a UV emission at 384 nm is originated from the exciton recombination corresponding to the near-band edge transition (NBE) of ZnO and less visible emissions peaks are observed at 413 nm, 432 nm, and 470 nm which correspond to violet and blue emission [15]. The violet band at 432 and 413nm were assigned to the recombination of an electron at Zinc interstitial and a hole in the valence band. The blue

band at 470nm is attributed to the recombination between the zinc interstitial (Zni) energy level to the zinc vacancy (Vzn) energy level, and approximately it is in agreement with the transition energy from Zni energy level to (Vzn) energy level [16]. Fig. 2 shows that the PL peak position of NBE in Dy doped ZnO films does not shift significantly with increasing Dy concentration, however the intensity of NBE emission decrease monotonically as the Dy concentration in ZnO thin film was increased [6].

### 3.3 Scanning electron microscopy analysis

Scanning electron microscopy was used to determine the microstructure of thin films. The morphology of pure ZnO and Dy doped ZnO thin films deposited by spin coating technique and annealed at 450°C as shown in Fig. 3. Fig. 3(a) can be described as a structure of very fine particles, whose mean diameter around 0.757µm, but this structure is not completely flat and looks like wrinkled structure [17]. Fig. 3(b-d) represents the Dy doped ZnO thin films. It can be seen that all films have a uniform and homogeneous root like morphology and with tiny nanoparticles [11, 18] and they had the longest diameter compared to all other samples respectively. The root like structures tightly bonded with increasing Dy concentration. During deposition, the layer of crystalline grains is built onto a glass substrate. Many particles were merged with other particles to make a long structure of ZnO which is called twisted root-like morphology [11].

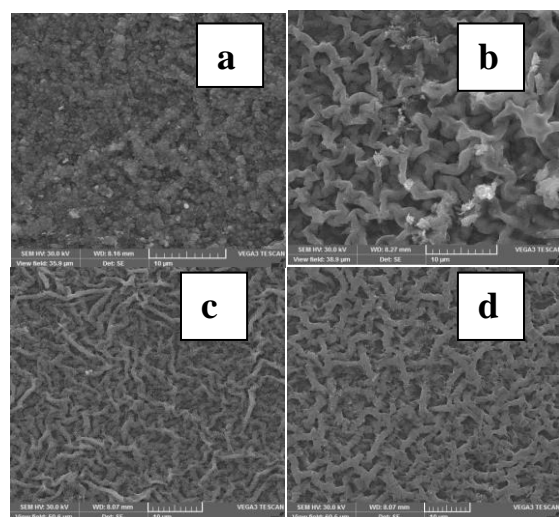


**Fig -3:** SEM images of (a) pure ZnO (b) 1% Dy: ZnO (c) 2% Dy: ZnO and (d) 3%Dy: ZnO thin films.

### 3.4 Energy dispersive X-ray analysis (EDX)

Chemical analyzes are consistent with these observations by the strong presence of O, Zn and Dy elements in all studied films [19]. EDX spectra of pure ZnO and Dy doped ZnO systems are shown in Fig. 4(a-d). Fig. 4(a) shows the peaks of Zn and O elements in pure ZnO and Fig. 4(b-d) shows the peaks of Zn, Dy and O elements for the doped (Zn<sub>1-x</sub>Dy<sub>x</sub>)O samples thus it allows us to study the effect of increasing Dy content on ZnO matrix [16]. The Dy doped ZnO films are only composed of Zn, O and Dy, which confirms the presence of dysprosium within the films.

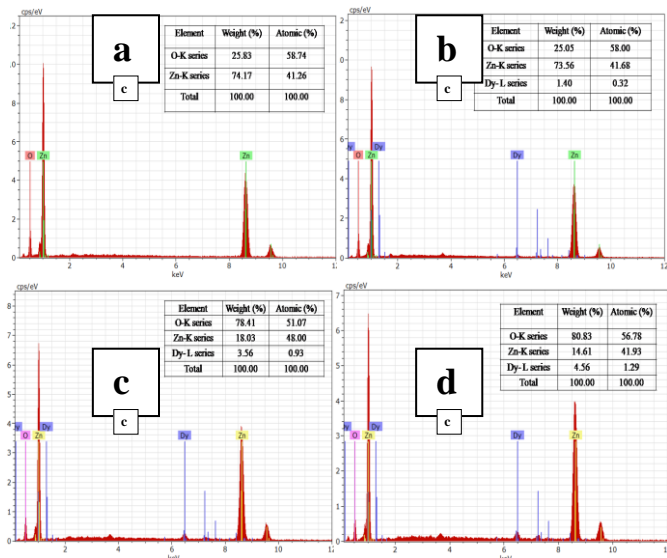


Fig -4: EDX spectrum of (a) pure ZnO (b) 1% Dy: ZnO (c) 2% Dy: ZnO and (d) 3% Dy: ZnO thin films.

### 3.5 UV -Vis Spectroscopy analysis

The absorption spectra of hierarchical structures of ZnO films deposited on a glass substrate with various concentration of Dysprosium nitrate such as 0%, 1%, 2% and 3% carried out in the wavelength range of 300-1100 nm were shown in Fig.5. It is absorbed that absorption edge slightly shifts towards higher wavelength region with an increase in the doping concentration [20] the spectra of films show a band gap absorbed edge at around 400 nm that results from the electron transition from the valance band to the conduction band [21].

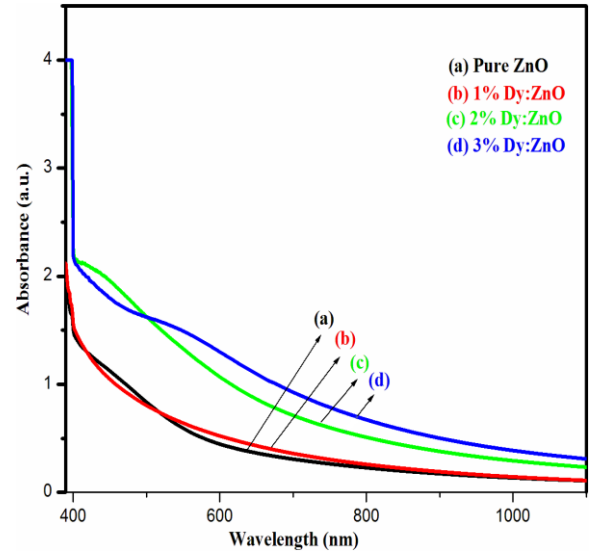


Fig -5: Optical absorption spectra of pure and Dy doped ZnO thin films

Fig.6 shows the transmittance spectra of ZnO films doped with different amounts of Dysprosium. All the films exhibit a low value of transmittance are found to be (7, 11, 34 and 40%) in the UV region [22] and visible range above 500nm [23]. The transmittance of the films decreases as a function of doping concentration caused by the scattering occurred in the films due to different defects [20].

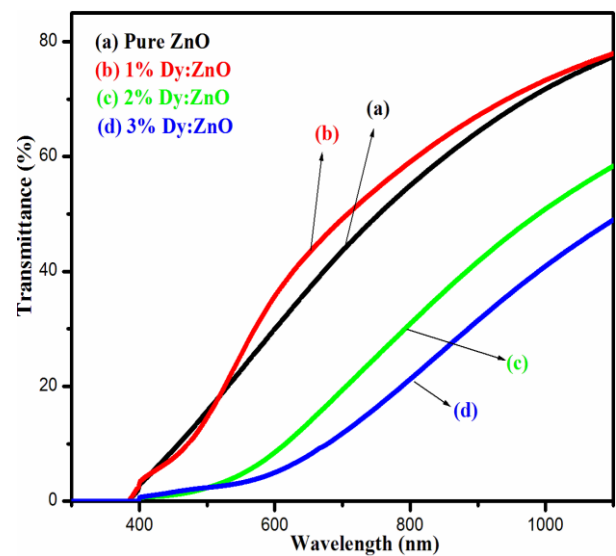


Fig-6: Transmittance spectra of ZnO thin films doped with different Dy concentration

The band gap of the pure and Dy doped ZnO thin films was estimated by extrapolation of the linear portion of  $(\alpha h\nu)^2$  versus photon energy  $(h\nu)$  as shown in fig. 3.7(a-d)

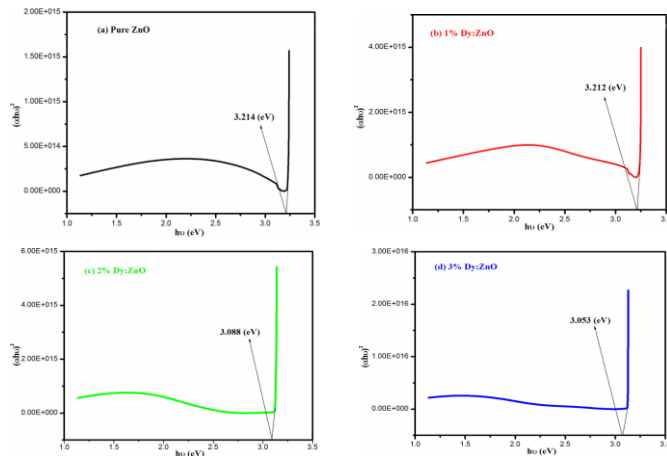


Fig -7: Band gap values of (a) Pure ZnO (b) 1% Dy: ZnO (c) 2% Dy: ZnO and (d) 3% Dy: ZnO thin films

The optical band gap energy decreases from 3.214 to 3.053eV with increasing Dy concentration, this decrease in band gap with an increase in Dy doping can be attributed to the sp-d spin exchange interaction between the band electrons and the localized d electrons of the Dy<sup>2+</sup> ions substituting Zn<sup>2+</sup> ions [15].

The optical parameters are a refractive index for application of ZnO films in optic communication applications. It is well known that the complex refractive index (n) of the films can be expressed by the following relation,

$$n = n(\lambda) + ik(\lambda)$$

The refractive index (n) of the films were calculated by the following relation,

$$n = \left( \frac{1 + R}{1 - R} \right) - \sqrt{\frac{4R}{(1 - R)^2} - k^2}$$

Where,

n is the refractive index (real part)

$k = \left( \frac{\alpha \lambda}{4\pi} \right)$  is extinction coefficient (imaginary part) and

R is the reflectance.

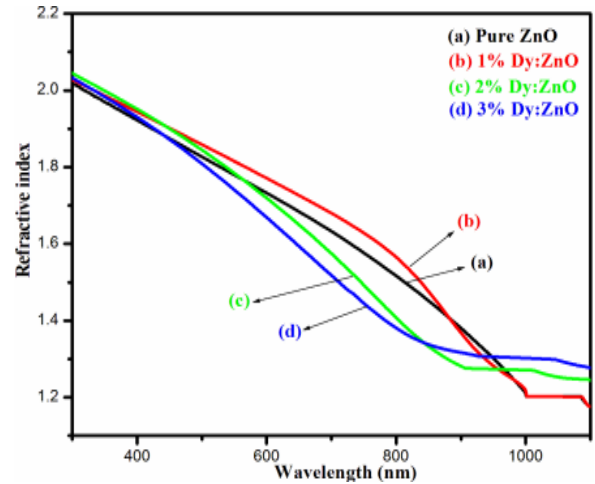


Fig -8: The variation of refractive index (n) of the pure and Dy doped ZnO thin films.

Fig. 8. shows the refractive (n) index of pure and Dy doped ZnO thin film with different Dy contents in the wavelength range of 300 to 1100 nm. The refractive index of all samples decreased with respect to wavelength. It can see that the n values increase with the increasing doping content. In general, the refractive index of ZnO single crystal is about 2.0 [24]. However, it was found that the average refractive index of all the obtained films in the visible range has been varied in the range of 2.01 to 2.04. The variation of the refractive index is with respect to the thickness of films. When the crystallite density is high in film, the light interaction is more on crystallites in the film. This leads to increase the refractive index of the film [25].

#### 4. CONCLUSIONS

Pure and Dy-doped (0.01, 0.02 and 0.03 at.%) ZnO thin films deposited on a glass substrate using sol-gel spin coating technique at constant 3000rpm for the 30s and annealed at 450°C. The XRD pattern showed that all the films are polycrystalline with hexagonal wurzite structure and preferentially oriented along the (101) growth planes. All the prepared films exhibited low magnitude of transmittance (10 to 40%) in the UV visible range and above 450nm, the optical band gap values decreased from 3.214 to 3.053 eV with increasing doping concentration whereas the average crystalline size decreased from 36.47 to 16.46nm. The PL spectra of ZnO and Dy doped films showed a broad and intensive peak at 384nm (violet emission) is more intense than the peaks at 432nm, 413nm (violet emission) and 470nm (blue emission). The SEM micrographs indicated that the pure ZnO films have wrinkle structure, and the doped ZnO films show homogeneous root-like morphology.

## One Day International Seminar on Materials Science &amp; Technology (ISMST 2017)

4<sup>th</sup> August 2017

Organized by

Department of Physics, Mother Teresa Women's University, Kodaikanal, Tamilnadu, India

## REFERENCES

- [1] D. Sharul Ashikin Kamruddin, Kah Yoong Chan, Ho Kwang Yow, Mohd Zainizan Sahdan, "Zinc oxide films prepared by sol-gel spin coating technique", *Appl. Phys. A*, 104, 2011, pp.263-268.
- [2] Amira Guesmi, Chaker Bouzidi, Habib Elhouichet, "Spectroscopic properties of Dy<sup>3+</sup> doped ZnO for white luminescence applications", *Spectrochim. Acta A*, S1386-1425, (17), pp. 30050-1.
- [3] J.T. Chen, J. Wang, F. Zhang, G.A. Zhang, Z.G. Wu, P.X. Z.G. Wu, P.X. Yan, "The effect of La doping concentration on the properties of zinc oxide films prepared by the sol-gel method", *J. Cryst. Growth*, 310, 2008, pp. 2627-2632.
- [4] P. Venkateswari, P. Thirunavukkarasu, T. Sivakumar, K. Shanmugasundram and C. Ramesh, "Characterization of the Zinc Oxide coated using Spin Coating Technique by FTIR", *J. Nanosci. Nanotechnol.*, 2, 2014, pp. 420-423.
- [5] Saliha Ilican, Mujdat Caglar, Yasemin Caglar, "Sn doping effects on the electro-optical properties of sol-gel derived transparent ZnO films", *Appl. Surf. Sci.*, 256, 2010, pp. 7204-7210.
- [6] R.S. Ajimsha, A.K.Das, B.N. Singh, P. Misra, L.M. Kukreja, "Structural, electrical and optical properties of Dy doped ZnO thin films grown by buffer assisted pulsed laser deposition", *Physica E*, 42, 2010, pp. 1838-1843.
- [7] Chien- Yie Tsay, Kai-shiung Fan Sih-Han Chen, Chia-Hao Tsai, "Preparation and Characterization of ZnO transparent semiconductor thin films by sol-gel method", *J. Alloy. Compd.*, 495, 2010, pp. 126-130.
- [8] R.S. Ajimsha, Amit. K. Das, M.P. Joshi, and L.M. Kukreja, "Quantum corrections to low temperature electrical conductivity in Dy doped ZnO thin films", *Thin Solid Films*, 589, 2015, pp. 521-525.
- [9] Ying Zhang and Dijiang Wen, "Infrared emission properties of RE (RE= La, Ce, Pr, Nd, Sm, Eu, Gd, Tb and Dy) and Mn co-doped Co<sub>0.6</sub>Zn<sub>0.4</sub>Fe<sub>2</sub>O<sub>4</sub> ferrites", *Mater. Chem. Phys.*, 131, 2012, pp. 575-580.
- [10] A. Babdyopadhyay, S. Modak, S. Acharya, A.K. Deb, P.K. Chakrabarti, "Microstructural, magnetic and crystal field investigations of nanocrystalline Dy<sup>3+</sup> doped zinc oxide", *Solid State Sci.*, 12, 2010, pp. 448-454.
- [11] Heri Sutanto, Sufwan Durri, Singgig Wibowo, Hady Hadiyanto, Eko Hidayanto, "Rootlike Morphology of ZnO:Al Thin Film Deposited on Amorphous Glass substrate by Sol-Gel Method", *Phys. Res. Inter.*, 87, 2016, pp. 1-7.
- [12] Ranuch Yayapao, Titipun Thongtem, Anukorm Phuruangrat, Somchai Thongtem, "Sonochemical synthesis of Dy-doped ZnO nanostructures and their photocatalytic properties", *J. Alloys Compd.*, 576, 2013, pp. 72-79.
- [13] C. Jayachandariah, K. Siva Kumar, G. Krishnaiah, N. Madhusudhana Rao, "Influence of Dy dopant on structural and photoluminescence of Dy- Doped ZnO nanoparticles", *J. Alloys. Compd.*, 623, 2015, pp. 248-254.
- [14] Ehmet Yilmaz, Sakir Aydogen, "The effect of Pb doping on the characteristic properties of spin coated ZnO thin films: Wrinkle structures", *Mater. Sci. Semicond. Process*, 10, 2015, pp. 162-170.
- [15] Mahroug, S. Boudjadar, S. Hamrit, L. Guerbous, "Structural, morphological and optical properties of Undoped and Co-doped ZnO thin films prepared by sol-gel process", *J.Mater. Sci: Mater. Electron.*, 25, 2014, pp. 4967-4974.
- [16] Arul Mary, J.Judith Vijaya, M. Bououdina, L. John Kennedy, J.H. Daie, Y. Song, "Investigation of structural, surface morphological, optical properties and first-principles study on electronic and magnetic properties of (Ce, Fe)-co doped ZnO", *Physica B*, 456, 2015, pp. 344-354.
- [17] Amia Znaidi, Tahar Touam, Dominique Vrel, Nacer Souded, Sana Ben Yahia and Ovidiu Brinza, "AZO Thin Films by Sol-Gel Process for Integrated Optics", *Coatings*, 3, 2013, pp. 126-139.
- [18] Aydin, H.M. El-Nasser, C. Aydin, Ahmed. A.Al-Ghamdi and F. Yakuphanoglu, "Synthesis and Characterization of nanostructured Undoped and Sn doped ZnO Thin Films via Sol-Gel Approach", *Appl. Surf. Sci.*, 14, 2016, 12-30.
- [19] Souissi, M. Amlouk and S. Gueemazi, "ZnO:Mo:In nanofilms on SiO<sub>2</sub> substrate under investigation framework of the second optical transition", *Opt. Mater.*, 64, 2017, pp. 502-511.

**One Day International Seminar on Materials Science & Technology (ISMST 2017)****4<sup>th</sup> August 2017****Organized by****Department of Physics, Mother Teresa Women's University, Kodaikanal, Tamilnadu, India**

---

- [20] V. Mohite, V.V. Ganbavle and K.Y. Rajpure, "Photoelectrocatalytic activity of immobilized Yb doped WO<sub>3</sub> photo catalyst for degradation of methyl orange dye", *J. Energy. Chem.*, 117, 2013, pp. 13825–13831
- [21] Guyen Minh Vuong, Nguyen Due Chinh, Bui The Huy and Yong-Ill Lee, "CuO- Decorated ZnO Hierarchical Nanostructures as Efficient and Established Sensing Materials for H<sub>2</sub>S Gas Sensors", *Scientific Reports*, 6, 2016, pp. 26736.
- [22] F. Hussein, Ghufuran Mohammad Shabeeb, S. Sh. Hashim, "Preparation ZnO Thin Film by using Sol-Gel processed and determination of thickness and study optical properties", *J. Mater. Environ. Sci.*, 2(4), 2011, pp. 423-426.
- [23] Saad. A. Jaber, Hussein F. Hussein and H. Bakr, "Synthesis and Effect of Thickness on the Structure and Optical Properties of Spin Coating method", *Sci. J. Phys.*, 2015, pp. 1-18.
- [24] W. Wang, F. Wu, D.X. Tian W.J.Li, L. Fang, C.Y. Kong and M. Zhou, " Effects of Na Content on structural and optical preparation of Na-doped ZnO thin films prepared by sol-gel method", *J. Alloys Compd.*, 623, 2015, pp. 367-373.
- [25] T.Marimuthu, N. Anandhan, R. Thangamuthu and S. Surya, "Influence of solution viscosity on hydrothermally grown ZnO thin films for DSSC application", *Superlattices*, 98, 2016, pp. 332-342.